agronomy

MDPI

Article

Drip Irrigation Soil-Adapted Sector Design and Optimal Location of Moisture Sensors: A Case Study in a Vineyard Plot

Jaume Arnó [1,*], Asier Uribeetxebarria [2], Jordi Llorens [1,3], Alexandre Escolà [1], Joan R. Rosell-Polo [1], Eduard Gregorio [1] and José A. Martínez-Casasnovas [4]

1 Research Group in AgroICT & Precision Agriculture, Department of Agricultural and Forest Sciences and Engineering, Universitat de Lleida—Agrotecnio CERCA Centre, Rovira Roure 191, 25198 Lleida, Spain; jordi.llorens@udl.cat (J.L.); alex.escola@udl.cat (A.E.); joanramon.rosell@udl.cat (J.R.R.-P.); eduard.gregorio@udl.cat (E.G.)
2 NEIKER-Basque Institute for Agricultural Research and Development, Berreaga 1, 48160 Derio, Spain; uribeetxebarria.asier@gmail.com
3 Serra Húnter Fellowship, Universitat de Lleida, 25003 Lleida, Spain
4 Research Group in AgroICT & Precision Agriculture, Department of Chemistry, Physics and Environmental and Soil Sciences, Universitat de Lleida—Agrotecnio CERCA Centre, Rovira Roure 191, 25198 Lleida, Spain; joseantonio.martinez@udl.cat
* Correspondence: jaume.arno@udl.cat; Tel.: +34-973-702859

Abstract: To optimise sector design in drip irrigation systems, a two-stage procedure is presented and applied in a commercial vineyard plot. Soil apparent electrical conductivity (ECa) mapping and soil purposive sampling are the two stages on which the proposal is based. Briefly, ECa data to wet bulb depth provided by the VERIS 3100 soil sensor were mapped before planting using block ordinary kriging. Looking for simplicity and practicality, only two ECa classes were delineated from the ECa map (*k*-means algorithm) to delimit two potential soil classes within the plot with possible different properties in terms of potential soil water content and/or soil water regime. Contrasting the difference between ECa classes (through discriminant analysis of soil properties at different systematic sampling locations), irrigation sectors were then designed in size and shape to match the previous soil zoning. Taking advantage of the points used for soil sampling, two of these locations were finally selected as candidates to install moisture sensors according to the purposive soil sampling theory. As these two spatial points are expectedly the most representative of each soil class, moisture information in these areas can be taken as a basis for better decision-making for vineyard irrigation management.

Keywords: irrigation zoning; ECa soil sensor; moisture sensors location; soil sampling; vine crop; irrigation sector design

Citation: Arnó, J.; Uribeetxebarria, A.; Llorens, J.; Escolà, A.; Rosell-Polo, J.R.; Gregorio, E.; Martínez-Casasnovas, J.A. Drip Irrigation Soil-Adapted Sector Design and Optimal Location of Moisture Sensors: A Case Study in a Vineyard Plot. *Agronomy* **2023**, *13*, 2369. https://doi.org/10.3390/agronomy13092369

Academic Editor: Pablo Martín-Ramos

Received: 31 July 2023
Revised: 7 September 2023
Accepted: 8 September 2023
Published: 12 September 2023

1. Introduction

Soil is a natural body that is spatially variable. Furthermore, soil also varies in depth and there are even highly dynamic soil properties that vary over time [1]. This adds greater uncertainty when it comes to reliably knowing the spatiotemporal pattern of soil variation. On the other hand, soil heterogeneity can occur at different spatial scales resulting in different soil properties within the same plot, whether large or small. This is especially common in fruit tree plantations and vineyards in many producing areas, with plots often less than one hectare, and where the impact of small-scale soil variability on crop growth and productivity may be important [2–6]. Focusing on irrigation, soil-adapted site-specific irrigation management may be a real option given the soil-crop relationship. However, managing irrigation at the plot level in this way requires a procedure (or protocol) that allows soil spatial variability to be assessed in those properties directly related to and/or influencing soil moisture content for optimal irrigation plot design.

A variety of sensors are currently available for farmers and technicians for soil water content (SWC) monitoring [7]. Problems with these moisture sensors are related to the low spatial sampling resolution commonly used (usually one sampling point per plot to control all sectors within the plot as a whole). So, while some areas within the plot edaphically fit the data provided by the moisture probes, others may not be optimally managed. On the other hand, in the framework of precision agriculture (PA), sensors to measure the soil apparent electrical conductivity (ECa) have been extensively tested and validated [8–10]. Galvanic contact resistivity (GCR) sensors and electromagnetic induction (EMI) sensors are the most used options [9]. To obtain usable data, electric current introduced or induced by the sensor should cover a soil volume reaching, at least, the depth explored by the crop roots. This means covering the wet soil depth in the drip irrigation systems installed in vineyards. The volume of soil wetted by the irrigation emitter can vary greatly in width and depth depending on soil type and irrigation management. In semi-arid areas of southern Europe, it is common to find wet bulb depths that usually vary from 60 to 150 cm. Hence the recommendation to keep the first meter in depth at approximately field capacity [11], installing moisture probes that measure to depths of 90 cm or more [12]. Two ECa measurements are usually provided by commercial sensors, of which the so-called deep-ECa allows the subsoil layer to be reached.

In the most efficient systems, ECa data are acquired continuously (on-the-go) and georeferenced using a global navigation satellite system (GNSS) receiver. Mapping this information (ECa map) is then a good starting point to characterise the soil and its variability [13]. In fact, there are many studies that show a significant spatial relationship between ECa and a number of soil properties [5,14], such as soil texture [15,16], soil water content [17], organic matter content [18], cation exchange capacity [19], and salinity [15] (the latter especially in semi-arid areas). Therefore, the use of ECa sensors and the resulting maps provide an indirect determination of soil characteristics [1] and, more importantly, allow spatial patterns of some soil properties linked to the SWC to be obtained [20,21] and used for zoning [22]. Often revealing boundaries of soil series with different properties [23], ECa maps thus provide valuable ancillary information for the design of irrigation systems in what can be called a "soil-based irrigation sector optimization strategy".

Plot zoning based on ECa maps using different classification methods has become a well-studied topic in recent years [24–28], with successful applications in vineyard [29] and other orchards [30]. Once the zoning process has been applied, spatially delimited zones often have different sizes and substantially irregular shapes. From this point of view, designing adapted soil-based irrigation sectors is challenging. In fact, it addresses a new disruptive concept by prioritizing the irrigation–soil binomial over seeking to design regular and identical sectors according to exclusively hydraulic criteria. Economically, with irrigation sectors adapted to soil variability, greater efficiency in water use and fertilizers should be achievable [31].

Location of moisture probes is not a minor issue. Assuming two soil classes within the plot, it is part of the design to decide on the optimal placement of at least two sets of humidity probes (sensors) for irrigation control. Optimal location of sensors is required so that measurements allow adequate control of the soil class (and therefore of linked irrigation sectors) they are monitoring. As this is a critical point [7], various methods to search for these optimal locations have been investigated in recent years. To cite a recent example, Bazzi et al. [32] developed an algorithm reporting the number of leaf sensors and their optimal locations (trees) to assist in precision irrigation. In the case study presented in this paper, purposive soil sampling [33] is the proposed approach to find these optimal locations.

Opportunities for site-specific management in vineyard plots have been thoroughly discussed [29,34–36]. In vineyards, improvements in irrigation scheduling have been proposed based on modelling the vine water status at different spatial scales [7,21]. However, real application of these models requires that irrigation sectors (management units for the farmer) adjust the spatial pattern of those soil properties (also including soil slope, soil

mulching and terrain relief as influential factors [37,38]) that generate the main source of variation in soil and crop moisture content. Adapting irrigation sectors to soil spatial variability is not a common practice, probably because there are few studies showing the advantage of applying variable-rate irrigation (VRI) based on irrigation prescription maps [39]. In fact, many winegrowers and irrigation managers are unaware of the possible use of ECa sensors to optimise the design of drip irrigation systems, with also a positive impact on the water footprint in the current agronomic context of climate change and drought. Faced with this situation, the Low Input Sustainable Agriculture (LISA) research project was recently completed with the aim of developing easy ECa data processing protocols to optimise the design of vineyard drip irrigation systems. A two-step procedure is presented in this work and applied in a commercial vineyard plot. Specifically, by using soil ECa data and purposive soil sampling, irrigation systems performance can be optimised based on (i) designing irrigation sectors adapted to soil zoning, and (ii) locating optimal sites within the plot where moisture sensors for irrigation control should be installed (smart points). The ultimate goal is to make more efficient use of water in drip irrigation systems that cover soils with different properties and with different requirements.

2. Materials and Methods

2.1. Study Area and Test Plot

The study area comprised a 14.5 ha plot located in Raimat (Lleida, NE Spain, 41°39′43″ N, 0°29′54″ E, Figure 1), planted with *Vitis vinifera* L. cv. Tempranillo from 1998 to 2015. The plot is sited in an area whose original materials are marls with interbedded sandstones and limestones of Tertiary origin. These materials have given rise to different soils that can be found in the plot according to the relief [40]: Typic Xerorthents, shallow soils with silt loam texture, located in the upper part of the plot with convex slope; Typic Xerorthents, moderately deep soils with silt loam texture located in the convex-rectilinear slopes connecting with the infilled bottom; and Typic Xerorthents and Fluventic Haploxerepts, deep soils with silty clay loam texture developed in the infilled bottom [41]. The average slope of the plot was 8.1 ± 3.4%, with a range between 0.2% (almost flat in the infilled bottom) and 19.8% (in the convex-rectilinear slope).

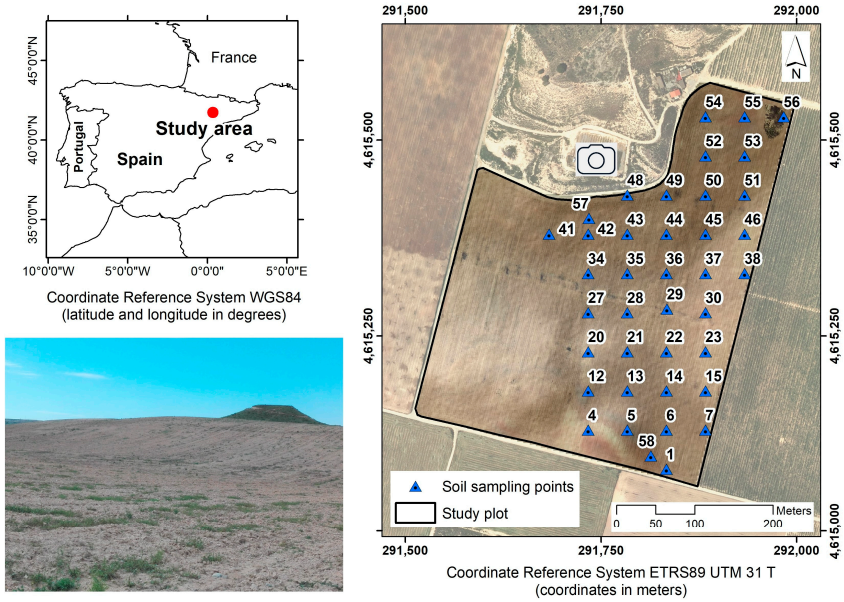

Figure 1. (**Top left**) location of the study area. (**Right**) study plot (size of 14.5 ha) with location of the soil sampling points. A shadow image showing the relief was overlaid to allow its interpretation. (**Bottom left**) photographic image of the study plot at the moment of the soil apparent electrical conductivity (ECa) survey. The position from which the photograph was taken is represented by a camera icon in the image on the right.

2.2. Outline of the Proposed Procedure

To solve the problem of adapting irrigation sectors to the soil spatial variability, the following methodological scheme is proposed (Figure 2). First, ECa data are acquired by means of an ECa surveyor, either of galvanic contact (Veris 3100 in the present case study) or electromagnetic induction. ECa mapping has proven effective in delimiting areas with rather clay soils and/or salinity problems in vineyard plots [42]. Then, ordinary block kriging is performed to create an ECa map (raster map). It is recommended that ECa measurements cover the expected depth of the wet bulb created by the irrigation emitters (deep-ECa for the VERIS surveyor). Alternatively, the user may consider using an ECa map focused primarily on the shallower topsoil if moisture from irrigation is concentrated in this layer [43]. However, as many sensors provide shallow and deep measurements of ECa, both maps can complement each other and be used together.

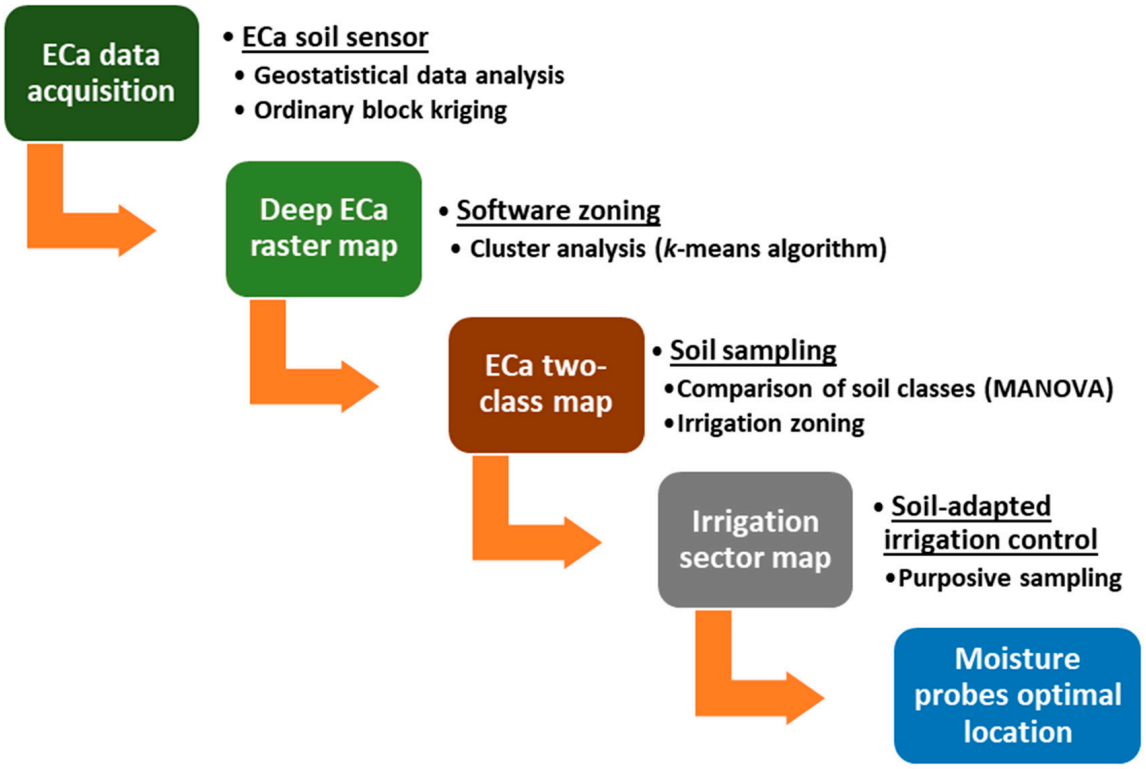

Figure 2. Flowchart of the proposed methodology for soil-adapted irrigation sector design and optimal location of moisture sensors at plot level.

In a second step, ECa data are clustered. The unsupervised *k*-means algorithm is used by setting the number of classes to only two (high and low ECa). Two not simple questions arise at this point. First, and for the sake of simplicity, delimiting only two ECa classes is considered a practical way to facilitate a better design of soil-adapted irrigation sectors. Indeed, other more complex scenarios are also possible (three or more classes), with the farmer's edaphic knowledge being a key factor in the final decision. Unless otherwise stated, establishing two ECa-classes is the initial proposal (Figure 2), which can be modified (thus increasing the number of classes) in plots with greater and proven soil heterogeneity. Another issue concerns the use of one or two ECa maps in the clustering algorithm. Since the *k*-means algorithm is intended for multivariate analysis, the procedure foresees using the two maps (shallow-ECa and deep-ECa) obtained from the soil sensor. But this is compatible with using only one map (deep-ECa in Figure 2) when, by recent surface tillage, the structure and spatial pattern of the topsoil may have been greatly affected. This has been the case of the plot under study.

The third step serves to assess the differences in soil properties between the two ECa classes. For that, soil sampling within each ECa class allows the two ECa classes to be globally contrasted through a multivariate analysis of variance (MANOVA). Based on these results, a proposal of irrigation sector design (irrigation sector map, step four) is made resulting in two types of irrigation sector as they are linked to two different soil classes (low or high ECa). Independent statistical tests (Student's *t*-tests) finally allow key soil properties linked to humidity, water retention, or soil water regime to be established to differentiate the two types of irrigation sector probably requiring different irrigation management. The fifth and final step is focused on establishing the optimal location of the moisture probes. Considering the most significant soil property in the previous tests, a purposive sampling analysis is carried out to decide on the best placement among the sampling points previously used to characterise the soil at the plot level. In what follows in this paper, points selected for this optimal location are named "smart points". The different procedures involved in each of the aforementioned steps are described in greater detail below.

2.3. Apparent Electrical Conductivity (ECa) Data Acquisition and Mapping

An ECa survey was conducted on 6 June 2018 to map the spatial distribution of the apparent soil electrical conductivity in the study plot. As has been mentioned, this information can be used to delineate potential management zones to optimise drip irrigation sectors for planned future vineyards. The interest of ECa measurements lies in the fact that certain soil properties (texture, moisture content, salinity, etc.) influence this parameter [9]. Therefore, ECa mapping allows soil spatial variability to be quantified and analysed by looking for possible soil spatial patterns associated with possible variations in one or more soil physical properties.

The survey was carried out with a Veris 3100 sensor (Veris Technologies Inc. Salina, KS, USA). This sensor (Figure 3) allows the ECa of the soil to be measured at two depths: superficial from 0 to 30 cm (shallow ECa) and deep from 0 to 90 cm (deep ECa). By applying a known voltage, an electrical direct current is transferred into the soil. The measurement of the voltage drop between the transmitting and the receiving coulters (electrodes) makes it possible to calculate the electrical resistivity and conductivity (Figure 3). The ECa data acquisition step requires the use of a data logger of the same instrument and brand (Veris 3100), making it possible to connect a GNSS receiver via an RS-232 serial port. Data are stored in a text file containing 5 columns: geographic coordinates (longitude and latitude), shallow ECa (mS/m), deep ECa (mS/m), and elevation (m). The transformation to projected coordinates Universal Transverse Mercator (UTM) makes it possible to add the coordinates X (m) and Y (m).

In the present study, data were collected along linear strips separated from each other at a distance of 12 m, as recommended by Veris Technologies Inc. Tractor speed was between 7 and 10 km/h, with a sampling frequency of 1 Hz. Data were georeferenced using a Trimble AgGPS332 (Trimble Inc., Westminster, CO, USA) GNSS receiver with SBAS EGNOS differential correction in geographic coordinates WGS84 (EPSG 4326). The original data file contained 6235 points. ECa values above or below ± 2.5 times the standard deviation (SD) were considered outliers and removed from the original data file according to the criteria of Taylor et al. [27]. The final ECa data set consisted of 6114 points, which represented a density of 420 points/ha (Figure 4).

Mapping of the ECa was performed following the two phases involved in a conventional geostatistical analysis. First, variographic analysis was performed obtaining the experimental variograms of both the shallow and deep ECa. The fitting of theoretical variogram models allowed parameters such as structural variance and range to be obtained in addition to checking for a possible nugget effect on the spatial data. The use of the former to assess the opportunity for differentiated management at the plot level would be interesting. In a second step, spatial interpolation (kriging) was performed. Due to the large amount of ECa data, block ordinary kriging based on local variograms was used to test the

hypothesis of quasi-stationarity that presumably occurs in plots of several hectares. In the present research, the software used to carry out the geostatistical analysis and interpolation was Variogram Estimation and Spatial Prediction with Error (VESPER) from the University of Sydney [44]. The blocks were 10 m × 10 m, projecting the interpolated values on a grid of 2 m × 2 m (spatial resolution of the raster map). The resulting maps are presented in Section 3.1.

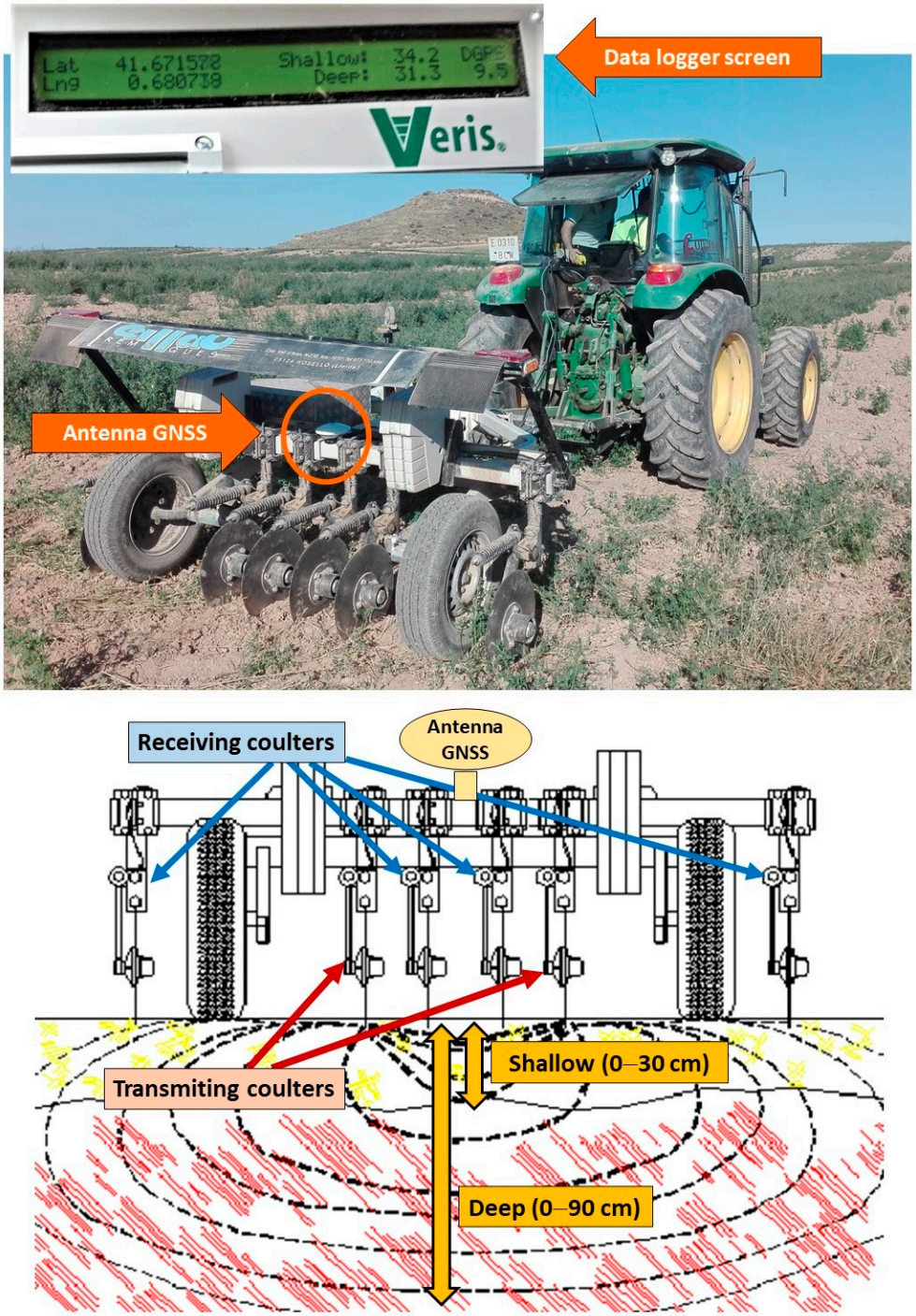

Figure 3. Veris 3100 ECa surveyor. Left: Image with detail of the location of the GNSS antenna; the data logger screen is also shown along with an example of shallow and deep ECa measurements. Right: Schematic representation of sensor operation.

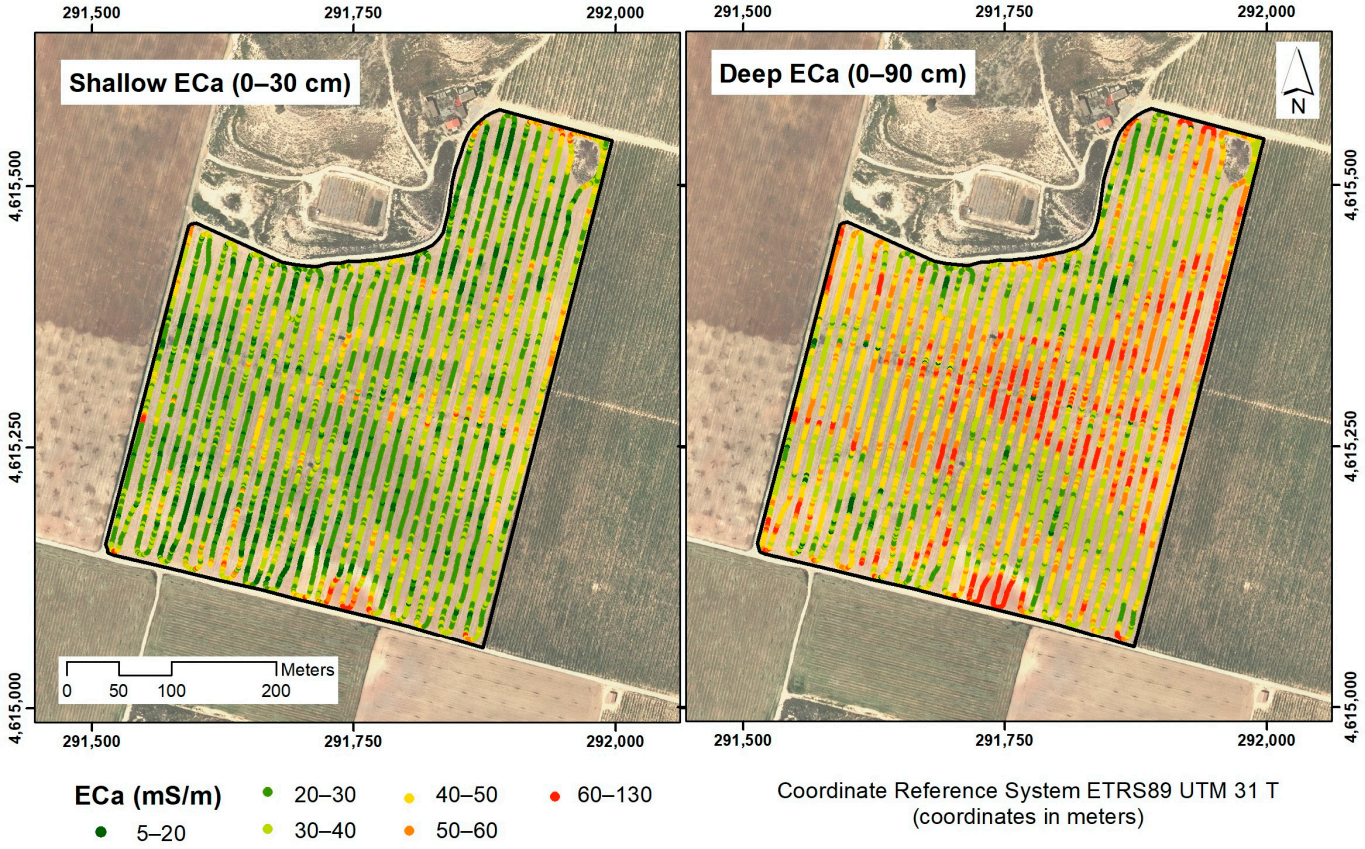

Figure 4. ECa points acquired with the Veris 3100 surveyor. Left: shallow ECa (0–30 cm). Right: deep ECa (0–90 cm).

2.4. Cluster Analysis

Cluster analysis based on the *k*-means algorithm was used to classify the pixels of the deep ECa map. The shallow ECa map was discarded because: (i) it presented a poorly structured spatial variation pattern (probably due to soil tillage prior to planting) with a much smaller variogram range and prominent nugget effect compared with the deep ECa data (see Section 3.1) and, fundamentally, (ii) it only measured ECa down to depths of 30 cm, which was very far from the expected depth of the typical irrigation wet bulbs in the area. The number of classes was set to two (low ECa and high ECa), as agreed with the estate managers who preferred a simple first approach to the problem of designing soil-adapted irrigation sectors. Without going into detail, the *k*-means algorithm is an unsupervised classification method that, in the present case, allowed pixels of the deep ECa raster map to be grouped into $k = 2$ groups or clusters. Initially, ECa pixels were randomly assigned to these two groups or classes. Then, through iteration, pixels were progressively reassigned until the sum of the squared differences between each pixel value and the centroid (mean value) of its group or cluster reaches a minimum. In this way, ECa pixels of one group were as similar as possible to each other but, at the same time, distant in terms of the ECa value contained in the pixels of the other group. Thus, the *k*-means algorithm allowed pixels to be classified into just two classes that managed to minimise the variability between pixels within the same class while maximizing the variability between classes. Management zone analyst (MZA) software was used for this task [45].

2.5. Soil Sampling and Multivariate Analysis to Contrast ECa Zoning and Irrigation

Differentiated management of irrigation and/or fertilization requires prior knowledge of the key soil properties that cause the spatial variability of ECa. For this reason, soil was first systematically sampled within each of the ECa classes and covering slightly more

than half of the plot (Figure 1). Then, in order to contrast the two ECa classes in terms of soil properties, a multivariate analysis of variance (MANOVA) was performed taking the ECa class as the factor under analysis and the soil sample properties playing the role of dependent variables. Compared with one-factor ANOVA, which applies to a single response variable, the MANOVA method allows contrasting differences between the levels of a certain factor (low ECa and high ECa) taking at the same time a set of response variables (vector of soil sampled variables). As only two levels of ECa were considered (low and high), equality of the two mean vectors corresponding to the two ECa classes was the null hypothesis to be tested. Thirty-nine (39) sampling points were arranged in a regular pattern of 50 m x 50 m and soils were sampled at 0–30 cm and 30–60 cm. The following properties were determined: pH (extract 1:2.5), electrical conductivity (EC) at 25 °C (extract 1:5), equivalent $CaCO_3$ (%), organic matter (OM) content (%), USDA textural fractions (%), and water retention capacity (WRC) at −33 kPa and −1500 kPa (%). In addition, another property considered in each sampling point was the slope (%), which was calculated from the digital elevation model of 5 m × 5 m produced by the Cartographic and Geologic Institute of Catalonia using the Slope function in ArcMap 10.7 (ESRI, Redlands, CA, USA).

Additionally, discriminant analysis of the sampling points was performed to check to what extent the points that fall within the two ECa classes were also discriminated in the same way but now based on the soil properties they contained. A high coincidence was expected assuming that ECa is a good tool for discriminating two very different soil classes. Establishing the final irrigation sector map was then simply a matter of defining the different irrigation sectors in size and shape to match the ECa variation pattern (or sectors spatially adapted to the two soil classes). At this stage of the procedure, we sought to obtain well-defined and compact sectors by refining the ECa class map. Statistical analyses in this section were performed using JMP® Pro 16.0.0 software.

2.6. Location of Moisture Probes through Purposive Sampling

In accordance with the procedure shown in Figure 2, the final step was to determine the optimal location to install the moisture probes for soil water content monitoring. Assuming that two soil classes can be differentiated within the plot (Sections 2.4 and 2.5), two sets of sensors (if different soil depths are monitored at the same site) should be installed in two representative locations to ensure proper monitoring and irrigation control. It was proposed to choose these locations from among the previously established soil sampling grid points (Figure 1). Two selection methods were possible: randomly choosing the two points (one per class) or purposely choosing the sites that best represented the two previously defined soil classes (in this case usually marking the locations based on the farmer's intuition or experience instead of choosing them on purpose but based on a more informed decision).

Figure 5 (adapted from Webster and Lark [33]) is used as an example to better understand the method behind purposive sampling. Assuming A and B represent the two ECa classes of the previously defined ECa two-class map, purposive sampling requires establishing a single soil property that, being significantly different according to the ECa class (which is to say according to the two types of irrigation sector), can also influence the irrigation management. To establish this reference soil property, a series of independent statistical tests (Student's *t*-tests) comparing the two types of irrigation sector were performed. The soil property that showed the lowest type I error (significance level adjusted by the Bonferroni correction) was finally used in the procedure. Adopting this soil property as our prediction variable (z), purposive sampling attempts to purposely search for the location within each ECa class whose actual value of z can also be considered as the most representative at the class level. To perform this (Figure 5), it is first necessary to determine the best predictor at the points marked with an empty circle (○) (i.e., any point inside the class), as well as the uncertainty of this prediction.

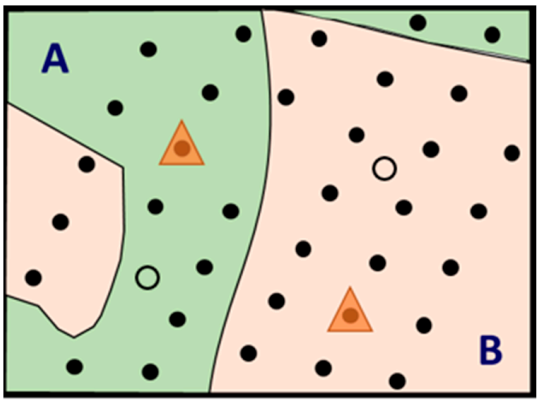

Figure 5. An example of an ECa class map of a rectangular plot (A-high ECa; B-low ECa). The black dots (•) represent soil sampling points over the plot to test for differences between classes. The empty circles (○) are locations where a prediction is required. The coloured triangles (Δ) are the purposively chosen sampling points as most representative of each class. The moisture probes should be installed in these locations. Figure adapted from Webster and Lark [33].

Considering no other information is available, the best predictor for a soil property z at i (point ○, Figure 5) within the class $k(k = A, B)$ is the mean of class k, μ_k. The uncertainty of such a prediction can be expressed in terms of the mean squared error, *MSE* (1):

$$MSE_k = E_i\left[(Z_{ik} - \mu_k)^2\right] = \sigma_k^2 \quad (1)$$

where σ_k^2 is the prediction variance, that is the variance within the corresponding stratum k. As the class mean is estimated by $\hat{\mu}_k$ (because μ_k is an unknown parameter), and may also be biased (if $\hat{\mu}_k$ is obtained from non-random sampling), Webster and Lark [33] suggest adding these two error sources to obtain the full squared prediction error (2):

$$MSE_k = \sigma_k^2 + var[\hat{\mu}_k] + bias^2[\hat{\mu}_k] \quad (2)$$

From a statistical optimization point of view, the goal is to install the moisture probes at those points within the plot where the *MSE* is minimised, which is to say the points that provide a reliable estimate of the class they represent. Taking the previous sampling covering the plot (or most of the two bounded classes within the plot) as the reference population, the farmer can randomly choose one of these points per class or, instead, deliberately choose a particular point per class among them. Using this last method for prediction, the z_{pk} values at the sites, p, chosen as representatives within each class (colored triangles in Figure 5, $k = A, B$) now replace the class means $\hat{\mu}_k$ as estimates of the variable at the prediction points (empty circles in Figure 5). Since the two points are set by the farmer (or advisor), it is true that $var\left[z_{pk}\right] = 0$ for each class (there is no source of variation in these values). However, the estimate is now biased at a value $d_k = z_{pk} - \mu_k$. Substituting the bias in (2) and taking the common within-class variance (σ_W^2) by assuming equally variable classes, the mean squared error of prediction can be assessed for the entire plot using (3):

$$\overline{MSE}_p = \sigma_W^2 + \sum_{k=1}^{K} a_k d_k^2, \quad (3)$$

where a_k is the area ratio of class k in the plot (or percentage of area occupied by class k).

Optimizing $\overline{MSE}_p$ to a minimum value, σ_W^2, can only be achieved by correctly choosing those sites where the values z_{pk} coincide with the class means μ_k. If the point per class is chosen randomly, it can be shown that the error becomes larger, specifically $2\sigma_W^2$. Assuming this range of error, our choice of sites for optimal sensor location is the one that meets the requirement $\sigma_W^2 < \overline{MSE}_p < 2\sigma_W^2$. To perform this, sites chosen as optimal locations were those that, for the soil property of interest, were as close as possible to the class means.

To verify that the inequality is true (and thus verify that choosing a point purposively by class is better than doing so randomly), the previous σ_W^2 and $\overline{MSE}_p$ were estimated using the sampling points in the field. Averaging over the two classes, $k = A, B$ (Figure 5), the average within-class variance was obtained by (4):

$$s_W^2 = \sum_{k=1}^{K} \sum_{i=1}^{n_k} (z_{ik} - \overline{z}_k)^2 / \sum_{k=1}^{K} (n_k - 1) \quad (4)$$

where n_k is the number of sampling points in k, and $\overline{z}_k$ is the mean. The prediction error was finally estimated using (5):

$$\widehat{MSE}_p = \frac{1}{N_V} \sum_{k=1}^{K} \sum_{v=1}^{V(k)} \left(Z_{vk} - z_{pk} \right)^2 \quad (5)$$

where z_{pk} is the value at the point chosen as representative within the class $k(k = A, B)$, Z_{vk} the value at the other sampled points acting as validation points and assuming they have been probabilistically chosen (there are $V(k)$ points depending on the class), and N_V the total number of validation points. More in-depth reasoning for purposive sampling can be found in Webster and Lark [33].

3. Results

3.1. ECa Maps

Figure 6 shows the interpolated ECa maps (shallow and deep) structurally classified in six classes using the same colour legend to facilitate visual interpretation. The values of the shallow ECa (0–30 cm) were clearly lower compared with the deep ECa (0–90 cm). According to Lund et al. [46], who established a correspondence between ECa values and soil textural fractions and salt content, ECa values measured in the plot were lower than the threshold indicating the presence of saline soils (about 100 mS/m). It is therefore expected that the spatial variation in ECa is probably related to other properties such as soil texture and/or soil water holding capacity. Based on previous knowledge of the soils in the plot (see Section 2.1), there is a correspondence between the ECa values and the soil classes present in the plot. Higher ECa values corresponded with the location of deep Typic Xerorthents and Fluventic Haploxerepts in the infilled bottom, and lower values corresponded with shallow or moderately deep Typic Xerorthents that appear in the upper part of the plot and in the convex-rectilinear slopes connecting with the infilled bottom.

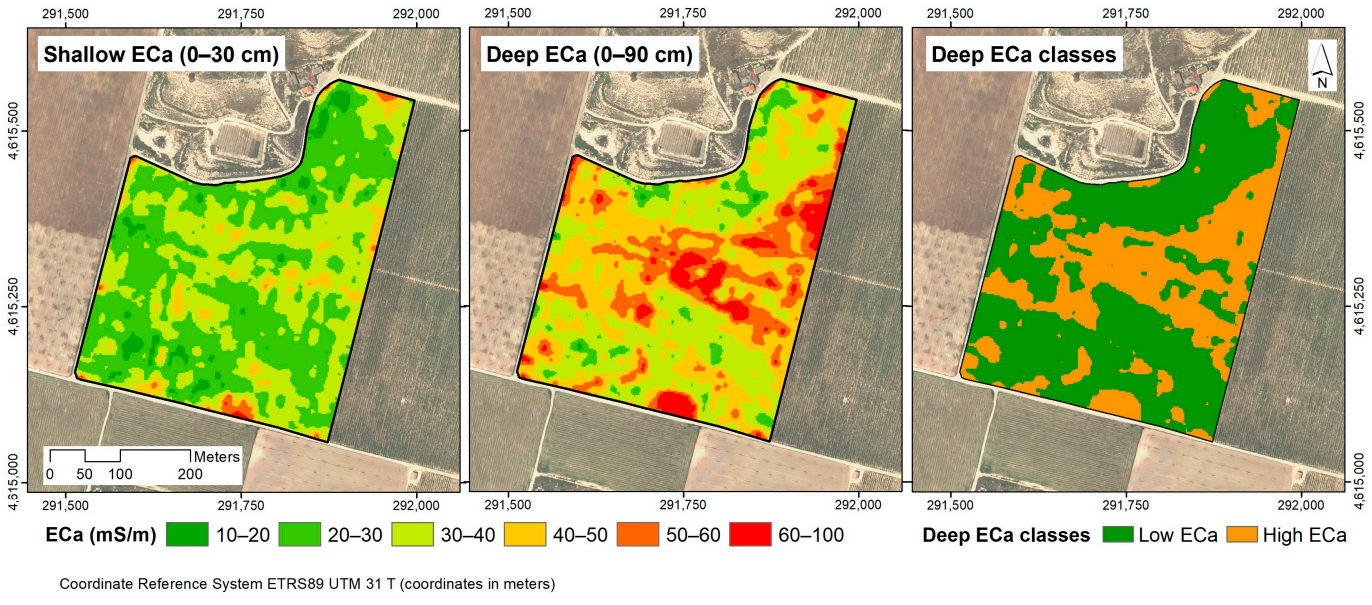

Figure 6. Left: Shallow ECa (0–30 cm) interpolated map. Centre: Deep ECa (0–90 cm) interpolated map. Right: Deep ECa cluster map showing two ECa classes (low and high ECa).

To create the ECa two-class map (*k*-means algorithm) on which the potential irrigation sectors are based, the deep ECa was chosen ahead of the shallow ECa (Figure 6—Right). As mentioned in the methodology, the justification for this decision is that a large part of the grapevine root system can be found in the top 100 cm of soil, with most of the fine roots between 10 and 60 cm [47]. The deep ECa ensures reaching this depth by integrating the response of soil properties up to 90 cm. The two ECa clusters showed significant differences in the Eca average values: 37.4 ± 5.0 mS/m and 53.6 ± 6.8 mS/m, respectively.

3.2. Multivariate Analysis of Variance (MANOVA) of Soil Properties According to ECa Clusters

According to Uribeetxebarria et al. [5], a separate analysis of variance (ANOVA) for each sampled soil property considering the two different levels of ECa may lead to misleading and inconsistent results. This is because ECa reflects the combined effect of soil properties as a whole and, for this reason, differences in soil should probably be verified using a multivariate approach (MANOVA). Thus, multivariate analysis (MANOVA) sought to check whether soils differed globally in its properties (jointly considering the two sampled depths) according to the spatial class of ECa, that is, according to the spatial location of the sampling points within the plot. Of the total available data (39 soil sampling points), four sampling locations were discarded since data for the sampling depth of 30 to 60 cm were not finally available at these points. Thus, a total of 35 effective sampling points were considered (Figure 7).

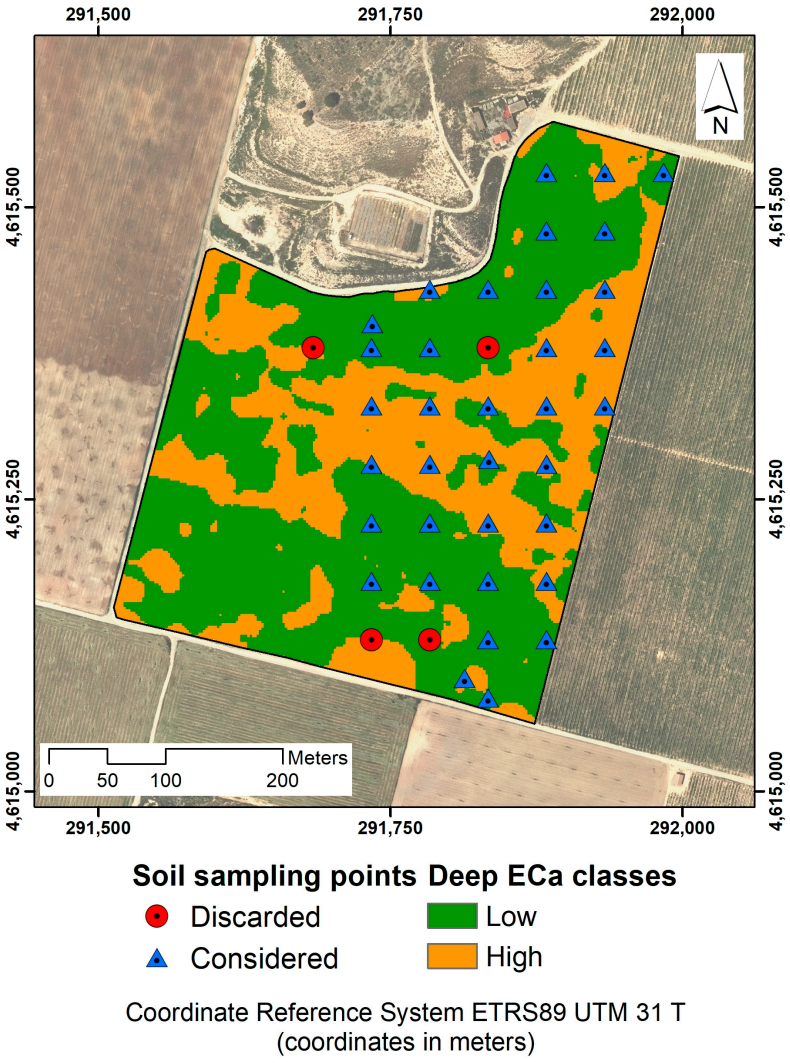

Figure 7. Deep ECa clusters and sampling points data set. The circle and red coloured points represent the discarded points for the MANOVA.

The result of the MANOVA was significant, with a p-value of 0.0365 for the statistic $F = \frac{(n_1+n_2-p-1)T^2}{(n_1+n_2-2)p}$ with p and $(n_1 + n_2 - p - 1)$ degrees of freedom, being n_1 and n_2 the sample sizes, T^2 the Hotelling's T^2 statistic and p the number of response variables included in the analysis (19 variables including soil properties at two depths and slope). Therefore, the two ECa clusters were able to differentiate two soils within the plot with particular soil and slope characteristics for each cluster. Figure 8 shows graphically the least squares mean values of soil properties discriminated by ECa cluster. Apparently, soil texture and slope are the most discriminated properties, emerging less sandy soils (or with finer textures) and flatter in areas within the high deep ECa class.

According to these results (Figure 8), it can be observed that the low and the high ECa classes can be distinguished by the silt content within the 0–30 cm layer, the sand content of both soil layers, and the clay content plus the WRC at −33 kPa within the 30–60 cm layer. In addition, the slope was also different between the two classes. This behaviour follows the principles of the interpretation of ECa data as described by several researchers [15,19], indicating that lower ECa values are related to higher sand content and higher values with the increase in finer texture particles. In addition, slope is related to soil depth because of the influence of this relief property in the erosion and deposition processes [48]. In the case of the study plot, lower slopes are found in the infilled bottoms, where deposition of finer soil particles from the connecting slopes occur. In contrast, shallower soils with higher sand content were found in areas with higher slope. On the other hand, since the sampling points are classified according to their soil properties into two groups that fully coincide with the ECa clusters (discriminant analysis not shown), there is no doubt that the ECa two-class map can be used as a reference for the optimised design of irrigation sectors.

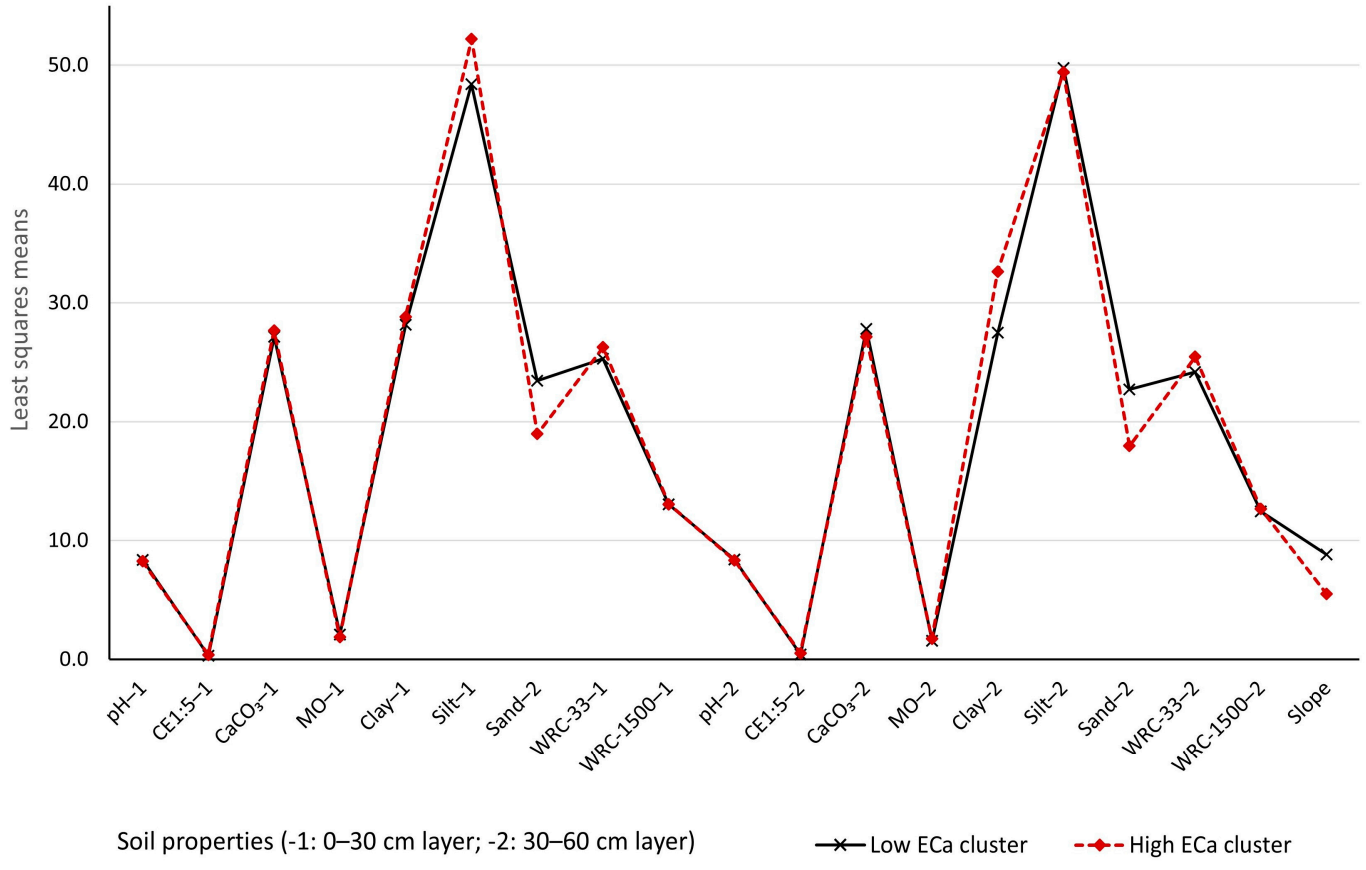

Figure 8. Least squares means of soil properties sampled by 0–30 cm and 30–60 cm soil layers for each ECa cluster.

3.3. Potential Irrigation Sectors and Location of Smart Points for Soil Moisture Content Monitoring

Based on the spatial distribution of the ECa clusters (Figure 6, right-hand side), 10 potential irrigation sectors were delineated, aiming to cover an average area per sector of about 1.50 ha, in accordance with owner criteria (Figure 9). Nevertheless, due to the irregular shape of the plot, the latter was not possible in all cases and different size sectors had to be delineated in some cases, with the smallest sector being 0.68 ha and the biggest 2.16 ha. Four sectors were designed covering the high ECa area and six within the low ECa area (Figure 9).

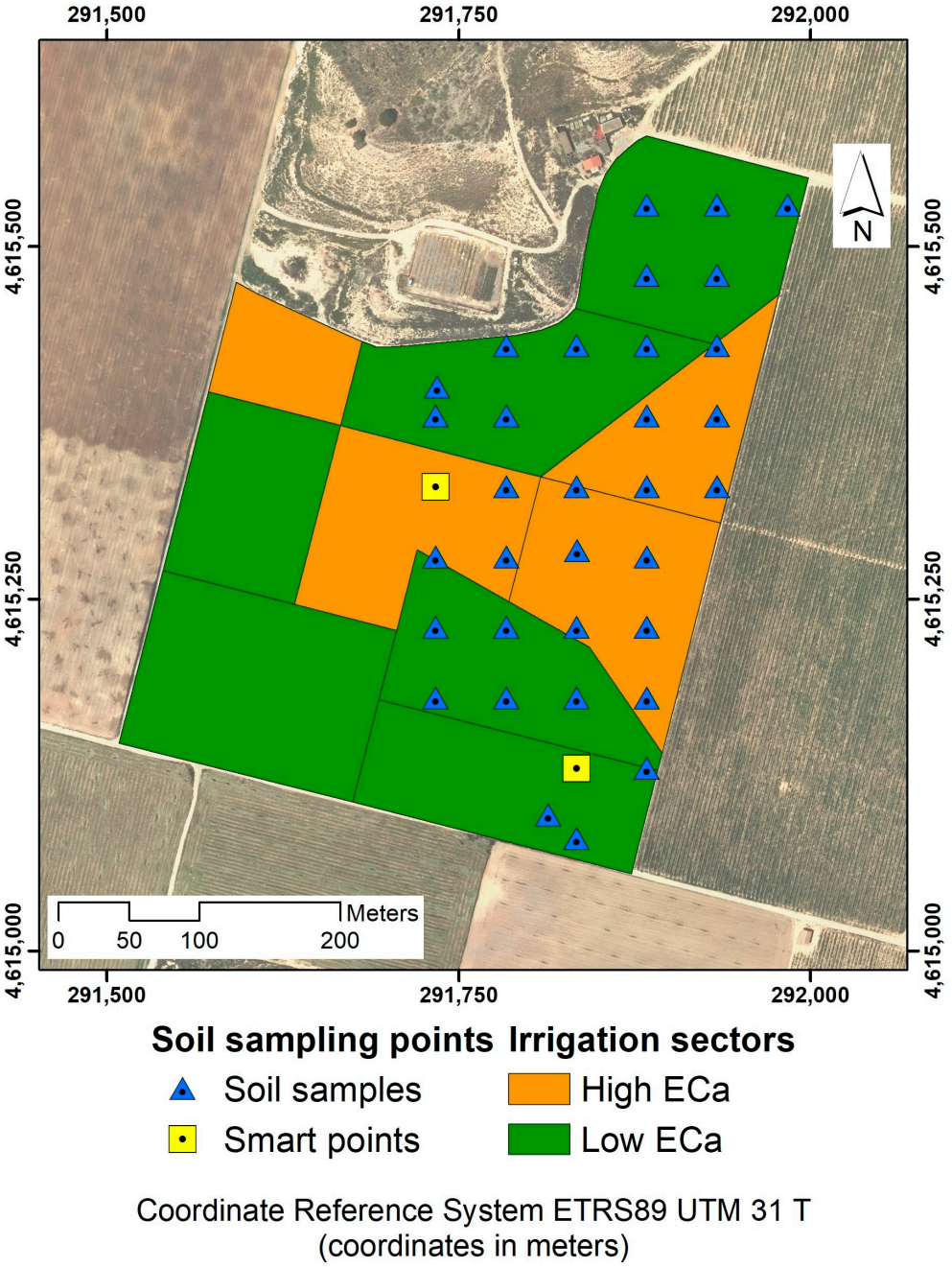

Figure 9. Potential irrigation sectors and soil sampling points considered for the identification of smart control points for soil moisture content monitoring. The square yellow points were the selected smart points resulting from the purposive sampling analysis.

Table 1 shows the average soil properties in each of the analysed soil layers for each type of irrigation sector (low and high ECa), together with the results of individual Student's t-tests in order to identify differences between irrigation sectors in terms of relevant soil properties. As there were some border sampling points that could have been included in another class of ECa with the delineation of the sectors, the mean values of Table 1 could vary a little from those displayed in Figure 8. In any case, the sector and not the ECa cluster should be the factor to consider in the analysis of the result of the irrigation design.

Table 1. Average soil properties in each type of the potential irrigation sectors. Total N = 35. Different upper-case and lower-case letters in rows indicate statistically significant differences between groups (low and high ECa irrigation sectors) at a p-value < 0.05, according to Student's t-tests (the upper-case and lower-case letters must be respectively compared between them) (see description of the acronyms in Section 2.5).

Soil Property	Irrigation Sectors with Low ECa (N = 20)		Irrigation Sectors with High ECa (N = 15)	
	0–30 cm	30–60 cm	0–30 cm	30–60 cm
pH	**8.37 a**	8.4 A	**8.27 b**	8.4 A
EC1:5	0.33 a	0.45 A	0.37 a	0.49 A
$CaCO_3$ (%)	27.3 a	27.5 A	27.5 a	27.5 A
OM (%)	2.2 a	1.5 A	1.8 a	1.9 A
Clay (%)	28.6 a	27.5 A	28.2 a	32.6 A
Silt (%)	**48.1 b**	50.2 A	**52.6 a**	48.9 A
Sand (%)	23.3 a	22.3 A	19.2 a	18.6 A
WRC–33 kPa (%)	25.1 a	24.4 A	26.5 a	25.3 A
WRC–1500 kPa (%)	13.1 a	12.5 A	13.1 a	12.6 A
Slope (%)	**9.1 a**		**5.1 b**	

In Table 1 it can be seen that no significant differences were obtained, except for pH for the first layer of soil, silt content, and slope. Of these properties, slope was the most significant (p-value < 0.0001), with a higher average value in the low ECa irrigation sectors (9.1%) compared with the high ECa sectors (5.1%). Silt content showed significant differences in the first soil layer, with higher content in the high ECa sector (p-value 0.0195). In contrast, sand content was lower in the high ECa sector (p-value 0.0993). As mentioned in Section 3.1, the predominant soils in the higher slope areas correspond to shallow Typic Xerorthents, with higher sand content than the soils located in the high ECa sectors. The latter mainly corresponded to deeper Typic Xerorthents and Fluventic Haploxerepts in the infilled bottom, which also had higher silt and clay content. Then, although statistically significant differences (p-value < 0.05) were only found for silt content and pH, a clear trend was observed, even in the 30–60 cm soil layer, in which higher clay content and lower sand content are more present in the high ECa sectors (Table 1). These results also confirm the relationships found in the MANOVA for soil texture and slope, thus confirming that the proposed map of irrigation sectors (Figure 9) is a feasible option for differentiated irrigation management.

The last step of the procedure referred to locating the moisture probes. As mentioned in Section 2.6, at least two sites (one for each sector type) are required to monitor soil water content and assist in irrigation control and scheduling. Taking into account Table 1 (where the results from 19 independent Student's t-tests are shown), the variable that showed the highest level of significance ($p < 0.0001$) was slope (%), which was also the only variable that could be considered significant according to the Bonferroni corrected level of significance ($p < 0.05/19 = 0.0026$). For this reason, it was decided to use slope as the reference soil property in the purposive sampling method to decide on the optimal location of the moisture probes. As in our method, a single variable was also used by Bazzi et al. [32] to obtain optimal locations for leaf sensors, in that case in two vines within each class.

The selected points were, for the infilled bottom area with the lowest global slope, the sampling point identified as 34, and, acting as a reference for the rest of the plot with

higher slopes probably associated with shallower and sandier soils, the point identified as number 6. Both locations (smart points) are shown in Figure 9 and the sampling points in Figure 1. The two sites meet the requirement of minimizing the slope prediction MSE for the plot as a whole. In this way, and given the low bias of both sites in relation to the corresponding class mean, slope values at these points provide the best possible estimate of the slope for any other location within the two irrigation classes. Furthermore, as expected, sites should be purposely chosen from among the sampling points and not randomly, as the corresponding prediction errors have shown (Table 2). On the other hand, the suitability of clustering into two ECa classes is also demonstrated by the coefficient of determination (R^2 = 0.53, Table 2) and, fundamentally, by verifying that $\widehat{MSE}_p$ is much lower than the prediction error ($s_T^2 + s_T^2/N$) when there is no classification and a single location for the moisture sensors is chosen at random to control plot irrigation.

Table 2. Prediction statistics for slope for the map of irrigation sectors.

			***MSE* of Prediction**		
	R^2	s_W^2	$\widehat{MSE}_p$	$2s_W^2$	$s_T^2 + s_T^2/N$
Slope (%)	0.53	3.468	3.475	6.936	7.59

R^2: coefficient of determination; s_W^2: pooled within-class variance or minimum value for the prediction error; $2s_W^2$: mean squared error for the entire plot using random sampling; $\widehat{MSE}_p$: mean squared error for the entire plot using purposive sampling; s_T^2: total variance of the N = 35 sampling points.

4. Discussion

The design of an irrigation system is a complex task due to the number of factors involved in the process [49]. In general, both agronomic design and hydraulic design are involved, the latter being a consequence of the former. From an agronomic point of view, knowing the soil–water–crop interrelation is key to establishing crop water requirements, especially for periods of greatest demand or maximum crop water stress. Once this has been specified, the sizing of irrigation units (sectors), pipes, pumping systems, and emitters per plant (in case of drip irrigation) is more of a hydraulic issue. Ultimately, the main objective is to supply water homogeneously with minimal pressure variations along and across the plot.

Although agronomic design is known to be fundamental (especially due to the soil-crop relationship), irrigation systems are often designed exclusively under hydraulic criteria. This is probably because the soil physical properties related to its water-holding capacity are costly to determine [50]. Furthermore, soil characterization is usually performed through composite samples (and much less so by adopting the basic and classic recommendation of taking four samples per hectare), thus ignoring the fact that the soil-water-crop relationship is site specific and possibly follows a pattern of spatial variation within the plot. In these cases, soil spatial variability is neglected and the opportunity to adapt irrigation sectors to soil property conditions is lost. Problems usually arise when watering with homogeneous doses for the whole plot, over-irrigating some parts and under-irrigating others, making the system inefficient. One example of this problem is given by Mirás-Avalos et al. [51], in which the irrigation sectors in a vineyard of 17.5 ha planted in 2018–2019 did not coincide with the spatial variability detected for soil water holding capacity and ECa. As a consequence, the vineyard owners opted for a more efficient irrigation adapted to the within-field soil spatial variability.

As already mentioned, adapting irrigation sectors to soil spatial variability is not usual. However, through the use of soil sensors to characterise soil spatial variability, it is expected that the current situation will gradually change as new PA technologies emerge [31]. Indeed, the application of on-the-go ECa soil sensors in agriculture is beginning to promote a change in the way soil information can be presented and analysed to meet the demands of using soil data at plot scales [52,53]. Different agricultural practices benefit from the information provided by ECa maps by varying seeding and fertilizer application rates, as well as soil characterization that can now be based on targeted sampling according

to ECa classes or zones [6,26,54]. In crop irrigation, trials have been undertaken on the use of ECa maps to delineate management zones for variable-rate irrigation in centre pivot irrigation systems [55–57]. In these systems, the irrigation chart can be adjusted by operating the centre pivot speed or sprinkler flow rate accordingly. However, this is not the case for sprinkler and drip irrigation systems used in vineyards and other tree crop plantations, where irrigation sectors are fixed and difficult to readjust if design errors are noticed at a later date. Since the life of a vineyard plantation can be estimated at 20 years or more [58], it can be assumed that an inadequate design of the system by not adapting the irrigation sectors to the soil may have important negative economic consequences. Taking into account the soil and its variability within the plot is therefore considered crucial in the design of fixed irrigation systems and, in particular, before making any decision on how irrigation sectors should be spatially dimensioned. Since there are no clear recommendations on this subject, a procedure that helps integrate soil information (ECa maps) in the initial design of pressurized irrigation projects becomes necessary for farmers and advisors in this sector.

In this paper, a two-stage procedure using ECa data and soil purposive sampling is proposed to better design drip irrigation systems in vineyard plots. The basic idea behind the method is to spatially zone soil ECa in two contrasting soil classes, and to then adapt irrigation sectors in size and shape to soil variation for better water management efficiency. Unlike other approaches that have mainly focused on arable crops under central pivot systems [56,57], the proposal made in the present study is, conceptually speaking, somewhat disruptive. In fact, it commits to moving from an irrigation design that uses exclusively hydraulic criteria to the design of sectors that make it possible to manage water according to site-specific requirements. As drip irrigation systems already in operation are difficult to modify, our option is different from those mentioned above, having to design the vineyard's irrigation system with the restrictions imposed by the soil within the plot. On the other hand, taking advantage of soil sampling extended over a certain plot area, the procedure also applies purposive sampling to identify two of the previous sampling points (smart points) for the optimal location of moisture probes. Making use of measurements from these sensors in these locations: (i) soil water content is monitored probably providing reliable mean measurements for each soil class (irrigation sector class), and (ii) irrigation rates and frequency can potentially be better adjusted.

However, drawbacks are also present. A first barrier to implementing this procedure is its potential economic cost. Farmers would have the additional cost of ECa surveying and mapping, soil sampling (which must have a sufficient density covering all or a large part of the plot area), laboratory analysis, and data processing. Therefore, initially resistant attitudes towards this technology can only be overcome by demonstrating the advantages of paying for an ancillary information such as ECa maps in order to optimise irrigation design. Undoubtedly, the role of irrigation advisors will be crucial for the success of protocols such as the one presented in this paper, managing to convince farmers that applying this new concept of soil-adapted irrigation sectors is the best option in terms of efficiency and sustainability. Unfortunately, there is presently little use of ECa soil sensors for this purpose due to the lack of awareness of such techniques in the irrigation sector. Nonetheless, we think that growers should consider using ECa maps as one more tool for decision making. They are aware that poorly designed irrigation systems in terms of sectorization are not usually changed until the end of the plantation life and, if it is decided that a readjustment is required, it is always technically complicated and economically expensive to make changes once the irrigation system is already operational.

The other issue that deserves discussion concerns the choice of location for the moisture probes. We recommend purposive sampling, seeking those points (one per class) where the reference soil property is closest to the class mean. This is relatively straightforward when a systematic sample of sufficient size like the one used in our protocol is available. However, in cases where systematic sampling can be avoided because the spatial distribution of soil classes is known in advance, choosing good representatives depends exclusively on

the experience of the observer [33]. Hence, where possible, a systematic sampling with a resolution adapted to the size of the plot should be performed. Another approach is to choose the location (among the sampling points) that presents a more restrictive value in terms of influencing the water stress of the crop. This would avoid watering based only on average values within the class, which can perhaps cause water deficit in areas that require applying irrigation in advance. This is a matter to be assessed and especially linked to the expected amount of common within-class variance (σ^2_W) (see Section 2.6).

Purposive sampling also puts into question that the choice of sites is based on a single soil property. In other work [32], researchers have also used a single piece of information (stem water potential (SWP)) on which to base the optimal placement of leaf sensors in almond orchards and vineyards. At first sight, in our case, using the slope instead of a soil property more closely associated to soil water content may seem surprising. However, since each location is characterized by a set of interrelated soil properties, it has been shown that, depending on the slope, the soil changes in depth and texture probably influence the soil water content in each site. This is important in terms of irrigation management, with the presence of sandier soils with steeper slopes in some sectors (low ECa class) allowing irrigation programming to be planned differently from that of other sectors (high ECa class) with lower slope and somewhat more clayey and possibly deeper soils. In short, differentiated irrigation management should focus on adapting the frequency of irrigation to the characteristics of the sector.

5. Conclusions

A spatially based sequenced procedure for using ECa maps as a source of soil information is proposed in order to optimise sector design in vineyard drip irrigation systems. Irrigation sectors are differentiated into two types linked to two soil classes (low and high ECa classes). In a later step, two sites are identified (one per class) to install moisture probes to monitor soil moisture and help in irrigation control. The procedure has proven to be satisfactory in a commercial plot planned for vineyard planting. Two issues are key for the procedure to be successful: (i) ECa acquisition at high resolution to then obtain ECa maps on which to base the plot zoning, and (ii) systematic soil sampling in a large part of the plot to compare the previously ECa classes in terms of properties related to soil moisture and water-holding capacity. Assuming two soils requiring specific irrigation management are contrasted within the plot, the size and shape of the irrigation sectors are then adjusted to the ECa spatial pattern (or soil spatial variability). Finally, taking advantage of the previous soil sampling, the suitability of purposely (instead of randomly) choosing two of the sampling points (smart points) as optimal locations for moisture probe sensors installation is demonstrated. In short, the use of ECa maps and a purposive sampling strategy can play a role in the design of irrigation systems, seeking to adapt sectors to within-field soil variability for better water use.

The proposed protocol contributes to a rational use of irrigation water in agriculture and to the sustainability of the production systems, particularly in semiarid regions where irrigation water can be a scarce resource. The fact that the irrigation sectors are designed according to the variability of soil properties, and probes are placed in locations representative of that variation, allows to better match the soil-crop binomial in terms of irrigation doses, irrigation scheduling and fertigation. As management of irrigation sectors is now site-specific, nutrient needs can also be applied at variable-rate doses contributing to the reduction in pollution of drainage and/or groundwater.

Some issues are pending further investigation. Specifically, the proposed procedure may need to be adapted to different conditions, as for example in cases where the relief does not play an important role (flat terrain) or in saline soils where the ECa values can be masked by the response of the salts. Plot zoning in more than two classes is another issue that, being closely linked to the spatial pattern of the ECa, remains open to the final decision of farmers and irrigation advisors. Also, selection of locations for moisture sensors can be simply directed, looking for average or extreme points, in cases where the

existing soil classes within the plot are already known, thus avoiding the cost of systematic soil sampling.

Author Contributions: Conceptualization, J.A. and J.A.M.-C.; methodology, J.A., J.A.M.-C. and A.U.; sampling, J.R.R.-P., J.L., E.G., J.A. and J.A.M.-C.; formal analysis, J.A. and J.A.M.-C.; writing—original draft preparation, J.A. and J.A.M.-C.; writing—review and editing, A.E., A.U., J.R.R.-P., J.L. and E.G.; figures, J.A. and J.A.M.-C.; supervision, J.A.; project administration, J.A. All authors have read and agreed to the published version of the manuscript.

Funding: This research was funded by ACCIÓ Generalitat de Catalunya, project COMRDI16-1-0031-06 (LISA: Low Input Sustainable Agriculture), within the COTPA RIS3CAT Community. Part of the funding came from the European Regional Development Fund (ERDF). In addition, part of the research is a result of the RTI2018-094222-B-I00 project (PAgFRUIT) funded by MCIN/AEI/10.13039/501100011033 and also by the ERDF.

Data Availability Statement: Data may be available by request to the corresponding author.

Acknowledgments: The authors appreciate participation in the LISA (Low Input Sustainable Agriculture) project [COMRDI16-1-0031], which has been promoted as a collaborative project (within the COTPA RIS3CAT Community) through the grouping of different companies from the wine sector and other fruit crops as well as research and innovation organizations in Catalonia (Spain).

Conflicts of Interest: The authors declare no conflict of interest.

References

1. Adamchuk, V.I.; Ferguson, R.B.; Hergert, G.W. Soil Heterogeneity and Crop Growth. In *Precision Crop Protection—The Challenge and Use of Heterogeneity*; Oerke, E.-C., Gerhards, R., Menz, G., Sikora, R.A., Eds.; Springer: Dordrecht, The Netherlands, 2010; pp. 3–16.
2. Käthner, J.; Zude-Sasse, M. Interaction of 3D soil electrical conductivity and generative growth in *Prunus domestica* L. *Eur. J. Hortic. Sci.* **2015**, *80*, 231–239. [CrossRef]
3. Pedrera-Parrilla, A.; Martínez, G.; Espejo-Pérez, A.J.; Gómez, J.A.; Giráldez, J.V.; Vanderlinden, K. Mapping impaired olive tree development using electromagnetic induction surveys. *Plant Soil* **2014**, *384*, 381–400. [CrossRef]
4. Unamunzaga, O.; Besga, G.; Castellón, A.; Usón, M.A.; Chéry, P.; Gallejones, P.; Aizpurua, A. Spatial and vertical analysis of soil properties in a Mediterranean vineyard soil. *Soil Use Manag.* **2014**, *30*, 285–296. [CrossRef]
5. Uribeetxebarria, A.; Arnó, J.; Escolà, A.; Martínez-Casasnovas, J.A. Apparent electrical conductivity and multivariate analysis of soil properties to assess soil constraints in orchards affected by previous parceling. *Geoderma* **2018**, *319*, 185–193. [CrossRef]
6. Uribeetxebarria, A.; Daniele, E.; Escolà, A.; Arnó, J.; Martínez-Casasnovas, J.A. Spatial variability in orchards after land transformation: Consequences for precision agriculture practices. *Sci. Total Environ.* **2018**, *635*, 343–352. [CrossRef]
7. Acevedo-Opazo, C.; Tisseyre, B.; Ojeda, H.; Ortega-Farias, S.; Guillaume, S. Is it possible to assess the spatial variability of vine water status? *OENO One* **2008**, *42*, 203–219. [CrossRef]
8. Adamchuk, V.I.; Hummel, J.W.; Morgan, M.T.; Upadhyaya, S.K. On-the-go soil sensors for precision agriculture. *Comput. Electron. Agric.* **2004**, *44*, 71–91. [CrossRef]
9. Corwin, D.L.; Lesch, S.M. Application of soil electrical conductivity to precision agriculture: Theory, principles, and guidelines. *Agron. J.* **2003**, *95*, 455–471. [CrossRef]
10. Mertens, F.M.; Pätzold, S.; Welp, G. Spatial heterogeneity of soil properties and its mapping with apparent electrical conductivity. *J. Plant Nutr. Soil Sci.* **2008**, *171*, 146–154. [CrossRef]
11. Buesa, I.; Pérez, D.; Castel, J.; Intrigliolo, D.S.; Castel, J.R. Effect of deficit irrigation on vine performance and grape composition of *Vitis vinifera* L. cv. Muscat of Alexandria. *Aust. J. Grape Wine Res.* **2017**, *23*, 251–259. [CrossRef]
12. Wilson, T.G.; Kustas, W.P.; Alfieri, J.G.; Anderson, M.C.; Gao, F.; Prueger, J.H.; McKee, L.G.; Alsina, M.M.; Sanchez, L.A.; Alstad, K.P. Relationships between soil water content, evapotranspiration, and irrigation measurements in a California drip-irrigated Pinot noir vineyard. *Agric. Water Manag.* **2020**, *237*, 106186. [CrossRef]
13. Carroll, Z.L.; Oliver, M.A. Exploring the spatial relations between soil physical properties and apparent electrical conductivity. *Geoderma* **2005**, *128*, 354–374. [CrossRef]
14. Kühn, J.; Brenning, A.; Wehrhan, M.; Koszinski, S.; Sommer, M. Interpretation of electrical conductivity patterns by soil properties and geological maps for precision agriculture. *Precis. Agric.* **2009**, *10*, 490–507. [CrossRef]
15. Corwin, D.L.; Lesch, S.M. Apparent soil electrical conductivity measurements in agriculture. *Comput. Electron. Agric.* **2005**, *46*, 11–43. [CrossRef]
16. Heil, K.; Schmidhalter, U. Characterisation of soil texture variability using the apparent soil electrical conductivity at a highly variable site. *Comput. Geosci.* **2012**, *39*, 98–110. [CrossRef]

17. Pedrera-Parrilla, A.; Van De Vijver, E.; Van Meirvenne, M.; Espejo-Pérez, A.J.; Giráldez, J.V.; Vanderlinden, K. Apparent electrical conductivity measurements in an olive orchard under wet and dry soil conditions: Significance for clay and soil water content mapping. *Precis. Agric.* **2016**, *17*, 531–545. [CrossRef]
18. Martinez, G.; Vanderlinden, K.; Ordóñez, R.; Muriel, J.L. Can apparent electrical conductivity improve the spatial characterization of soil organic carbon? *Vadose Zone J.* **2009**, *8*, 586–593. [CrossRef]
19. Sudduth, K.A.; Kitchen, N.R.; Wiebold, W.J.; Batchelor, W.D.; Bollero, G.A.; Bullock, D.G.; Clay, D.E.; Palm, H.L.; Pierce, F.J.; Schuler, R.T.; et al. Relating apparent electrical conductivity to soil properties across the north-central USA. *Comput. Electron. Agric.* **2005**, *46*, 263–283. [CrossRef]
20. Bramley, R.G.V. Understanding variability in winegrape production systems. 2. Within vineyard variation in quality over several vintages. *Aust. J. Grape Wine Res.* **2005**, *11*, 33–45. [CrossRef]
21. Acevedo-Opazo, C.; Tisseyre, B.; Guillaume, S.; Ojeda, H. The potential of high spatial resolution information to define within-vineyard zones related to vine water status. *Precis. Agric.* **2008**, *9*, 285–302. [CrossRef]
22. Fulton, A.; Schwankl, L.; Lynn, K.; Lampinenm, B.; Edstrom, J.; Prichard, T. Using EM and VERIS technology to assess land suitability for orchard and vineyard development. *Irrig. Sci.* **2011**, *29*, 497–512. [CrossRef]
23. Brogi, C.; Huisman, J.A.; Pätzold, S.; von Hebel, C.; Weihermüller, L.; Kaufmann, M.S.; van der Kruk, J.; Vereecken, H. Large-scale soil mapping using multi-configuration EMI and supervised image classification. *Geoderma* **2019**, *335*, 133–148. [CrossRef]
24. Córdoba, M.A.; Bruno, C.I.; Costa, J.L.; Peralta, N.R.; Balzarini, M.G. Protocol for multivariate homogeneous zone delineation in precision agriculture. *Biosyst. Eng.* **2016**, *143*, 95–107. [CrossRef]
25. Moral, F.J.; Terrón, J.M.; Marques da Silva, J.R.M. Delineation of management zones using mobile measurements of soil apparent electrical conductivity and multivariate geostatistical techniques. *Soil Tillage Res.* **2010**, *106*, 335–343. [CrossRef]
26. Peralta, N.R.; Costa, J.R. Delineation of management zones with soil apparent electrical conductivity to improve nutrient management. *Comput. Electron. Agric.* **2013**, *99*, 218–226. [CrossRef]
27. Taylor, J.A.; McBratney, A.B.; Whelan, B.M. Establishing management classes for broadacre grain production. *Agron. J.* **2007**, *99*, 1366–1376. [CrossRef]
28. Vitharana, U.W.A.; Van Meirvenne, M.; Simpson, D.; Cockx, L.; De Baerdemaeker, J. Key soil and topographic properties to delineate potential management classes for precision agriculture in the European loess area. *Geoderma* **2008**, *143*, 206–215. [CrossRef]
29. Ortega-Blu, R.; Molina-Roco, M. Evaluation of vegetation indices and apparent soil electrical conductivity for site-specific vineyard management in Chile. *Precis. Agric.* **2016**, *17*, 434–450. [CrossRef]
30. Aggelopoulou, K.; Fountas, S.; Pateras, D.; Nanos, G.; Gemtos, T. Soil spatial variability and site-specific fertilization maps in an apple orchard. *Precis. Agric.* **2011**, *12*, 118–129. [CrossRef]
31. Martínez-Casasnovas, J.A.; Arnó, J. Soil Sensors to Optimize Irrigation Zoning. In *Dossier Tècnic. Agricultura de Precisió: Aplicacions al Reg*; De Ribot, M.J., Malet, I., Teixidó, A., Cuadros, R., Sisquella, M.T., Vallverdú, X., Eds.; Generalitat de Catalunya, Departament d'Agricultura, Ramaderia, Pesca i Alimentació: Barcelona, Spain, 2020; Volume 107, pp. 32–36. (In Catalan)
32. Bazzi, C.L.; Schenatto, K.; Upadhyaya, S.; Rojo, F.; Kizer, E.; Ko-Madden, C. Optimal placement of proximal sensors for precision irrigation in tree crops. *Precis. Agric.* **2019**, *20*, 663–674. [CrossRef]
33. Webster, R.; Lark, R.M. *Field Sampling for Environmental Science and Management*; Routledge: London, UK; New York, NY, USA, 2013.
34. Arnó, J.; Martínez-Casasnovas, J.A.; Ribes-Dasi, M.; Rosell, J.R. Precision Viticulture. Research topics, challenges and opportunities in site-specific vineyard management. *Span. J. Agric. Res.* **2009**, *7*, 779–790. [CrossRef]
35. Bramley, R.G.V.; Hamilton, R.P. Understanding variability in winegrape production systems. 1. Within vineyard variation in yield over several vintages. *Aust. J. Grape Wine Res.* **2004**, *10*, 32–45. [CrossRef]
36. Tisseyre, B.; Ojeda, H.; Taylor, J. New technologies and methodologies for site-specific viticulture. *J. Int. Sci. Vigne Vin* **2007**, *41*, 63–76. [CrossRef]
37. Muršec, M.; Leveque, J.; Chaussod, R.; Curmi, P. The impact of drip irrigation on soil quality in sloping orchards developed on marl—A case study. *Plant Soil Environ.* **2018**, *64*, 20–25. [CrossRef]
38. Nouri, H.; Stokvis, B.; Galindo, A.; Blatchford, M.; Hœkstra, A.Y. Water scarcity alleviation through water footprint reduction in agriculture: The effect of soil mulching and drip irrigation. *Sci. Total Environ.* **2019**, *653*, 241–252. [CrossRef]
39. Ortuani, B.; Facchi, A.; Mayer, A.; Bianchi, D.; Bianchi, A.; Brancadoro, L. Assessing the effectiveness of variable-rate drip irrigation on water use efficiency in a vineyard in Northern Italy. *Water* **2019**, *11*, 1964. [CrossRef]
40. Dalurzo, H.C. Régimen Hídrico Del Suelo Y Producción de Viñas Bajo Diferentes Sistemas de Riego en Raimat (Lleida, España). Ph.D. Thesis, University of Lleida, Lleida, Spain, 2010. Available online: http://hdl.handle.net/10803/8249 (accessed on 26 March 2023).
41. Soil Survey Staff. *Keys to Soil Taxonomy*, 12th ed.; USDA-Natural Resources Conservation Service: Washington, DC, USA, 2014.
42. Rodríguez-Pérez, J.R.; Plant, R.E.; Lambert, J.-J.; Smart, D.R. Using apparent soil electrical conductivity (EC_a) to characterize vineyard soils of high clay content. *Precis. Agric.* **2011**, *12*, 775–794. [CrossRef]
43. Serrano, J.; Mau, V.; Rodrigues, R.; Paixão, L.; Shahidian, S.; Marques da Silva, J.; Paniagua, L.L.; Moral, F.J. Definition and validation of vineyard management zones based on soil apparent electrical conductivity and altimetric survey. *Environments* **2023**, *10*, 117. [CrossRef]

44. Minasny, B.; McBratney, A.B.; Whelan, B.M. *VESPER, Version 1.62*; Australian Centre for Precision Agriculture, McMillan Building A05, The University of Sydney: Camperdown, NSW, Australia, 2006.
45. Fridgen, J.J.; Kitchen, N.R.; Sudduth, K.A.; Drummond, S.T.; Wiebold, W.J.; Fraisse, C.W. Management zone analyst (MZA): Software for subfield management zone delineation. *Agron. J.* **2004**, *96*, 100–108. [CrossRef]
46. Lund, E.D.; Colin, P.E.; Christy, D.; Drummond, P.E. Applying soil electrical conductivity to precision agriculture. In *Proceedings of the Fourth International Conference on Precision Agriculture, St. Paul, MN, USA, 19–22 July 1998*; Robert, P.C., Rust, R.H., Larson, W.E., Eds.; ASA-CSSA-SSSA: Madison, WI, USA, 1999; pp. 1089–1100.
47. Hunter, J.J.; Archer, E.; van Schalkwyk, D.; Strever, A.; Volschenk, C. Grapevine roots: Interaction with natural factors and agronomic practices. *Acta Hortic.* **2016**, *1136*, 63–80. [CrossRef]
48. Morgan, R.P.C.; Quinton, J.N.; Smith, R.E.; Govers, G.; Poesen, J.W.A.; Auerswald, K.; Chisci, G.; Torri, D.; Styczen, M.E. The European Soil Erosion Model (EUROSEM): A dynamic approach for predicting sediment transport from fields and small catchments. *Earth Surf. Process. Landf.* **1998**, *23*, 527–544. [CrossRef]
49. Rodríguez Díaz, J.A.; Perea, R.G.; Moreno, M.A. Modelling and Management of Irrigation System. *Water* **2020**, *12*, 697. [CrossRef]
50. Shwetha, P.; Varija, K. Soil Water Retention Curve from Saturated Hydraulic Conductivity for Sandy Loam and Loamy Sand Textured Soils. *Aquat. Procedia* **2015**, *4*, 1142–1149. [CrossRef]
51. Mirás-Avalos, J.M.; Fandiño, M.; Rey, B.J.; Dafonte, J.; Cancela, J.J. Zoning of a Newly-Planted Vineyard: Spatial Variability of Physico-Chemical Soil Properties. *Soil Syst.* **2020**, *4*, 62. [CrossRef]
52. Scull, P.; Franklin, J.; Chadwick, O.A.; McArthur, D. Predictive soil mapping: A review. *Prog. Phys. Geogr.* **2003**, *27*, 171–197. [CrossRef]
53. Martínez-Casasnovas, J.A.; Arnó, J.; Escolà, A. Sensores de Conductividad Eléctrica Aparente Para el Análisis de la Variabilidad del Suelo en Agricultura de Precisión. In *Tecnología Hortícola Mediterránea. Evolución Y Futuro: Viveros, Frutales, Hortalizas Y Ornamentales*; Namesny, A., Conesa, C., Martín, L., Papasseit, P., Eds.; Biblioteca de Horticultura, SPE3 S.L.: Valencia, Spain, 2022; pp. 521–542.
54. Corwin, D.L.; Lesch, S.M.; Segal, E.; Skaggs, T.H.; Bradford, S.A. Comparison of Sampling Strategies for Characterizing Spatial Variability with Apparent Soil Electrical Conductivity Directed Soil Sampling. *J. Environ. Eng. Geophys.* **2010**, *15*, 147–162. [CrossRef]
55. Haghverdi, A.; Leib, B.G.; Washington-Allen, R.A.; Ayers, P.D.; Buschermohle, M.J. Perspectives on delineating management zones for variable rate irrigation. *Comput. Electron. Agric.* **2015**, *17*, 154–167. [CrossRef]
56. Yari, A.; Madramootoo, C.A.; Woods, S.A.; Adamchuk, V.I.; Huang, H.H. Assessment of Field Spatial and Temporal Variabilities to Delineate Site-Specific Management Zones for Variable-Rate Irrigation. *J. Irrig. Drain. Eng.* **2017**, *143*, 04017037. [CrossRef]
57. Serrano, J.; Shahidian, S.; Marques da Silva, J.; Paixão, L.; Moral, F.; Carmona-Cabezas, R.; Garcia, S.; Palha, J.; Noéme, J. Mapping Management Zones Based on Soil Apparent Electrical Conductivity and Remote Sensing for Implementation of Variable Rate Irrigation—Case Study of Corn under a Center Pivot. *Water* **2020**, *12*, 3427. [CrossRef]
58. Carbone, A.; Quici, E.; Pica, G. The age dynamics of vineyards: Past trends affecting the future. *Wine Econ. Policy* **2019**, *8*, 38–48. [CrossRef]